Solar Glare Hazard Analysis Tool (SGHAT) Technical Reference Manual

Clifford K. Ho, Cianan A. Sims, Julius Yellowhair, and Evan Bush
Sandia National Laboratories
(505) 844-2384, ckho@sandia.gov
SAND2014-18360 O
March 2015

Contents

1. Requirements

- Use of this software requires the latest version of one of the following free web browsers: Mozilla Firefox or Google Chrome.
- The Solar Glare Hazard Analysis Tool (SGHAT) can be accessed by registering at www.sandia.gov/glare.

2. Introduction

With growing numbers of solar energy installations throughout the United States, glare from photovoltaic (PV) arrays and concentrating solar systems has received increased attention as a real hazard for pilots, air-traffic control personnel, motorists, and others. Sandia has developed a web-based interactive tool that provides a quantified assessment of (1) when and where glare will occur throughout the year for a prescribed solar installation, (2) potential effects on the human eye at locations where glare occurs, and (3) an estimate of the maximum annual energy production.

The Solar Glare Hazard Analysis Tool (SGHAT) employs an interactive Google map where the user can quickly locate a site, draw an outline of the proposed PV array, and specify observer locations or paths. Latitude, longitude, and elevation are automatically recorded through the Google interface, providing necessary information for sun position and vector calculations. Additional information regarding the orientation and tilt of the PV panels, reflectance, environment, and ocular factors are entered by the user.

If glare is found, the tool calculates the retinal irradiance and subtended angle (size/distance) of the glare source to predict potential ocular hazards ranging from temporary after-image to retinal burn. The results are presented in a simple, easy-to-interpret plot that specifies when glare will occur throughout the year, with color codes indicating the potential ocular hazard. The tool can also predict relative energy production while evaluating alternative designs, layouts, and locations to identify configurations that maximize energy production while mitigating the impacts of glare.

This Technical Reference Manual describes the theory and models used in SGHAT.

3. Assumptions and Limitations

Below is a list of assumptions and limitations of the models and methods used in SGHAT:

- The software currently only applies to flat reflective surfaces. For curved surfaces (e.g., focused mirrors such as parabolic troughs or dishes used in concentrating solar power systems), methods and models derived by Ho et al. (2011) [1] can be used and are currently being evaluated for implementation into future versions SGHAT.
- When enabled, PV array single- or dual-axis tracking does not account for backtracking or the effects of panel shading and blocking.

- SGHAT does not rigorously represent the detailed geometry of a system; detailed features such as gaps between modules, variable height of the PV array, and support structures may impact actual glare results. However, we have validated our models against several systems, including a PV array causing glare to the air-traffic control tower at Manchester-Boston Regional Airport and several sites in Albuquerque, and the tool accurately predicted the occurrence and intensity of glare at different times and days of the year.

- SGHAT assumes that the PV array is aligned with a plane defined by the total heights of the coordinates outlined in the Google map. For more accuracy, the user should perform runs using minimum and maximum values for the vertex heights to bound the height of the plane containing the solar array. Doing so will expand the range of observed solar glare when compared to results using a single height value.

- SGHAT does not consider obstacles (either man-made or natural) between the observation points and the prescribed solar installation that may obstruct observed glare, such as trees, hills, buildings, etc.

- The variable direct normal irradiance (DNI) feature (if selected) scales the user-prescribed peak DNI using a typical clear-day irradiance profile. This profile has a lower DNI in the mornings and evenings and a maximum at solar noon. The scaling uses a clear-day irradiance profile based on a normalized time relative to sunrise, solar noon, and sunset, which are prescribed by a sun-position algorithm [2] and the latitude and longitude obtained from Google maps. The actual DNI on any given day can be affected by cloud cover, atmospheric attenuation, and other environmental factors.

- The ocular hazard predicted by the tool depends on a number of environmental, optical, and human factors, which can be uncertain. We provide input fields and typical ranges of values for these factors so that the user can vary these parameters to see if they have an impact on the results. The speed of SGHAT allows expedited sensitivity and parametric analyses.

4. Determination of Glare Occurrence

Determination of glare occurrence requires knowledge of the following: sun position, observer location, and the tilt, orientation, location, extent, and optical properties of the modules in the solar array. Vector algebra is then used to determine if glare is visible from the prescribed observation points.

4.1   Sun Position

The sun position algorithm[2] calculates the sun position in two forms: first as a unit vector extending from the Cartesian origin toward the sun, and second as azimuthal and altitudinal angles. The algorithm relies on the latitude, longitude and time zone offset from UTC in order to determine the position of the sun at every time step throughout the year.

First, we calculate the solar time:

$$t_{solar} = 4(L_{st} - L_{loc}) + E + t_{standard}$$

Where:

$$L_{st} = tz_{offset} * 15$$

$$E = 229.2(0.000075 + 0.001868 * \cos B - 0.0320077 * \sin B - 0.014615 * \cos 2B - 0.04089 * \sin 2B)$$

L_{st} is the local standard meridian, L_{loc} is the given longitude and E is the equation of time, in minutes.

The solar time can then be used to calculate the Hour angle, ω:

$$\omega = \Delta t_{noon} * 15$$

Where Δt_{noon} is the difference between solar time and solar noon.

Once the declination, δ is known, the solar zenith and azimuthal angle of the sun can be found:

$$\delta = 23.45 * \sin\left(360 * \frac{284 + n}{365}\right)$$

$$\theta_z = \cos^{-1}(\cos \varphi * \cos \delta * \cos \omega + \sin \varphi * \sin \delta)$$

$$\gamma_s = sign(\omega) \left| \cos^{-1}\left(\frac{\cos \theta_z \sin \phi - \sin \delta}{\sin \theta_z \cos \phi}\right) \right|$$

Where:

- n is the day of the year (1 to 365)

- θ_z is the sun zenith angle (subtract from 90 to get the altitude angle, θ_a)

- φ is the given latitude

- γ_s is the sun azimuthal angle

The sun altitude and azimuth can be converted to unit vector components as follows:

$$\vec{s_i} = \cos \theta_a * \sin \gamma_s$$

$$\vec{s_j} = \cos \theta_a * \cos \gamma_s$$

$$\vec{s_k} = \sin \theta_a$$

4.2 Reflected Sun Vector

Once the sun position is known for each time interval a simple vector reflection equation [4] can determine the reflected sun vector, based on the normal vector of the PV array panels:

$$x_1' - x_0 = v - 2(v \cdot \hat{n})\,\hat{n}$$

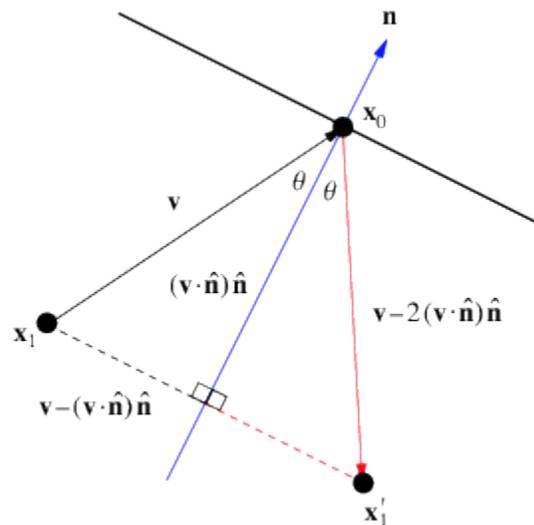Figure 1 illustrates this vector reflection graphically.

Figure 1 - Vector reflection over normal vector of plane. Source: mathworld.wolfram.com/Reflection.html

4.3 Scattering and Subtended Beam Angle

The reflected sun vector defines the axis of a conical beam representing the actual beam of sunlight. This sunbeam is translated to extend from the OP toward the PV array. The aperture of this conical sun beam is equivalent to β, the subtended beam angle, which is the sum of the sun shape and the scattering caused by slope error:

$$\beta = 2 * \left(\frac{\theta_{sun\ angle}}{2} + 2 * 3 * \theta_{slope\ error} \right)$$

4.4   Beam Projection onto PV Array Plane

The beam is projected onto the PV array in several steps: first, points lying on the edge of the beam in a conical section orthogonal to the axis are calculated. This conical section is arbitrarily defined to be 1 meter from the cone apex (the OP).

These 30 points are calculated by randomly generating two coordinates and solving for the third using the following equation:

$$v_{axis} \cdot v_{radius} = 0$$

This equation states that the cone axis is orthogonal to the radius vectors of the conical section upon which the 30 conical points lie.

Next, conical edge vectors are defined by subtracting the cone apex (the OP) from the cone points. This collection of vectors extends from the OP toward the PV array plane. These vectors define the conical sun beam. At their center, or the axis of the cone, is the reflected sun vector calculated in 4.2.

These conical vectors are then intersected with the PV array plane. This cone-plane intersection will be an elliptical conical section defined by 30 co-planar points.

These intersection points are calculated using line-plane intersection equations [5]:

$$d = \frac{(\boldsymbol{p_0} - \boldsymbol{I_0}) \cdot \vec{\boldsymbol{n}}}{\boldsymbol{I} \cdot \vec{\boldsymbol{n}}}$$

$$(x, y, z) = d\boldsymbol{I} + \boldsymbol{I_0}$$

Where:

- $\vec{\boldsymbol{n}}$ is the PV array panel normal vector

- $\boldsymbol{I}$ is one of the vectors extending from the OP to the PV array plane, which define the conical sun beam.

- $\boldsymbol{I_0}$ is a point on the vector (the OP)

- $\boldsymbol{p_0}$ is a point on the PV array plane

- d is the distance from the OP to the intersection point, and

- (x, y, z) define the intersection point for this vector.

The n intersection points found using the above equations define the elliptical conical section of the sun beam cone as it intersects the PV array plane.

Glare is present and viewable from the OP if any of the PV array vertices lie within this co-planar ellipse. This is determined using an optimized points-in-polygon algorithm from matplotlib [6].

4.5 PV Single-Axis Tracking

Single-axis tracking allows for the PV panels to rotate over one dimension in order to track the apparent movement of the sun over time. This rotation is modeled using the normal vector of the PV array panels, $\vec{n}$. The components of $\vec{n}$ are calculated using the following:

- β_t – Tracking axis tilt where 0º is parallel with flat ground and 90º is perpendicular to the ground, facing the horizon.

- μ – Panel offset from the tracking axis.

- ρ – Tracking, or rotation, angle designating the rotation of the panel at a given time. Clockwise and counter-clockwise over the tracking axis (see below).

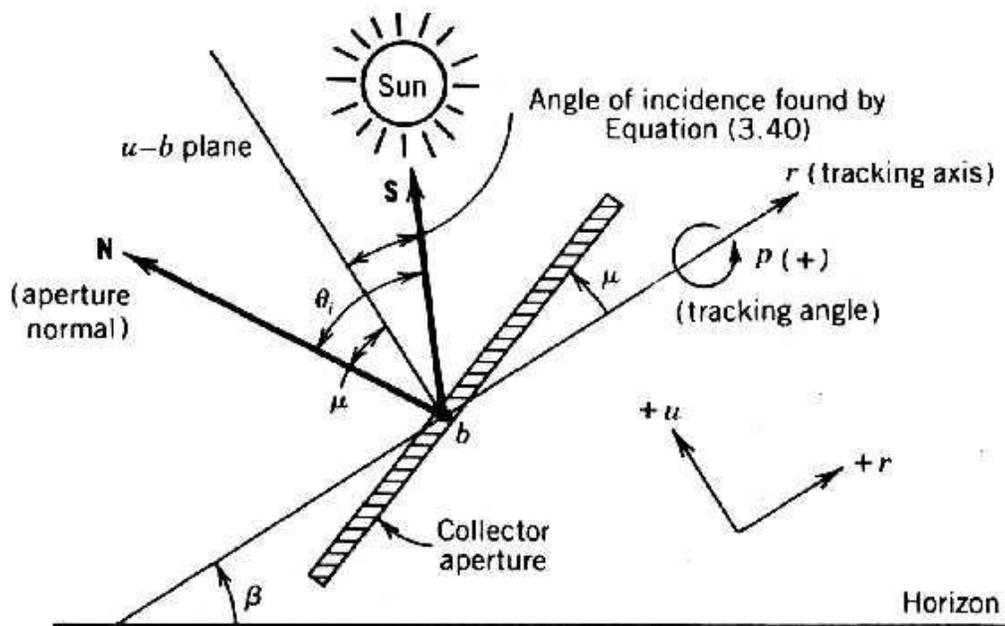- γ – Orientation of the tracking axis. Clockwise from due south (0º).

Figure 2 - PV panel with single-axis tracking. The panel normal is displayed as N. Source: http://www.powerfromthesun.net/Book/chapter04/chapter04.html

The components of $\vec{n}$ are first calculated in a Cartesian coordinate system of (*b, r, u*) where *r* aligns with the tracking axis, *b* is perpendicular to it and extends to the horizon, and *u* is perpendicular to *r* vertically (see Figure 2). Note that β_t, μ, γ are all inputs provided by the user.

$$\rho = \tan^{-1}\left\{\frac{\cos(\theta_a)\sin(\gamma_s - \gamma)}{\sin(\theta_a - \beta_t) + [1 - \cos(\gamma_s - \gamma)]\sin(\beta_t)\cos(\theta_a)}\right\}$$

$$\vec{n}_b = \sin\rho$$

$$\vec{n}_r = \sin\mu$$

$$\vec{n}_u = \cos\rho$$

These components are converted back to the standard Cartesian system:

$$\vec{n}_z = \vec{n}_u\cos\beta_t + \vec{n}_r\sin\beta_t$$

$$\vec{n}_e = -\vec{n}_u\sin(\gamma)\sin(\beta_t) + \vec{n}_b\cos(\gamma) + \vec{n}_r\sin(\gamma)\cos(\beta_t)$$

$$\vec{n}_n = -\vec{n}_u\cos(\gamma)\sin(\beta_t) - \vec{n}_b\sin(\gamma) + \vec{n}_r\cos(\gamma)\cos(\beta_t)$$

Vector components are calculated for the panels at each time step.

4.6 PV Dual-Axis Tracking

Dual-axis tracking implies the PV panels face "toward" the sun at every time step. Again, the panel normal varies every minute. Because the variance occurs in two dimensions, the sun vector (extending from the origin toward the sun) can be used as the panel normal:

$$\vec{n} = \vec{s}$$

5. Determination of Ocular Impact

Determination of the ocular impact requires knowledge of the direct normal irradiance, PV module reflectance, size and orientation of the array, optical properties of the PV module, and ocular parameters. These values are used to determine the retinal irradiance and subtended source angle used in the ocular hazard plot [1, 3].

5.1 Ocular Hazard Plot

The ocular impact of viewed glare can be classified into three levels based on the retinal irradiance and subtended source angle: low potential for after-image, potential for after-image, and potential for permanent eye damage [1, 3]. The following log-log plot illustrates these three areas of glare intensity:
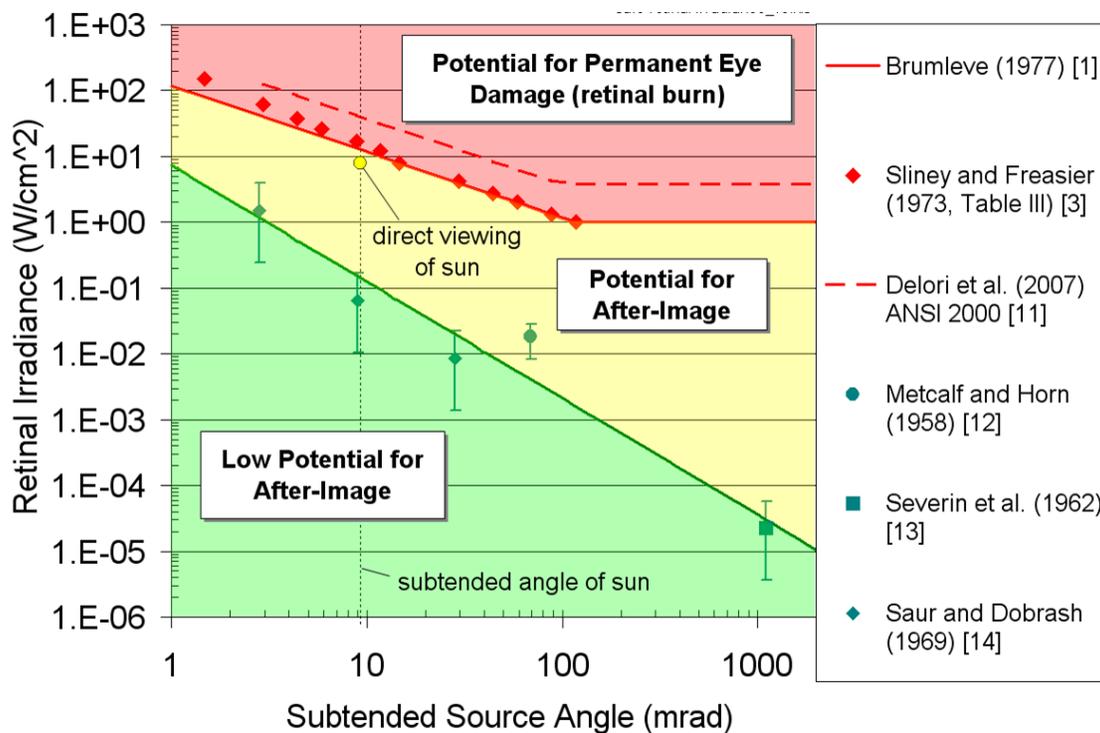

Figure 3 - Glare hazard plot illustrating the ocular impact as a function of retinal irradiance and subtended source angle [1, 3].

The subtended source angle represents the size of the glare viewed by an observer, while the retinal irradiance determines the amount of energy impacting the retina of the observer. Larger source angles can result in glare of high intensity, even if the retinal irradiance is low.

The boundary between the "yellow" and "red" regions, signifying glare that transitions from causing an after-image to causing permanent eye damage, can be quantified with the following equations:

$$E_{r,burn} = \frac{0.118}{\omega} \quad \text{for} \quad \omega < 0.118 \text{ rad}$$

$$E_{r,burn} = 1 \quad \text{for} \quad \omega \geq 0.118 \text{ rad}$$

The second boundary, between the low potential for after-image (green) and potential for after-image (yellow) areas, adheres to the following equation:

$$E_{r,flash} = \frac{3.59 \times 10^{-5}}{\omega^{1.77}}$$

5.2   Direct Normal Irradiance (DNI)

The variable direct normal irradiance (DNI) feature (if selected) scales the user-prescribed peak DNI using a typical clear-day irradiance profile. This profile has a lower DNI in the mornings and evenings and a maximum at solar noon. The scaling uses a clear-day irradiance profile based on a normalized time relative to sunrise, solar noon, and sunset, which are prescribed by a sun-position algorithm [2] and the latitude and longitude obtained from Google maps.

$$DNI = \cos(1 - t_s)$$

Here t_s represents the normalized time relative to solar noon. Normalization is based on the amount of time between sunrise or sunset and solar noon.

The DNI scaling profile was determined by fitting empirical DNI data to the cosine function, as illustrated in Figure 4. Note that DNI on any given day can be affected by cloud cover, atmospheric attenuation, and other environmental factors.
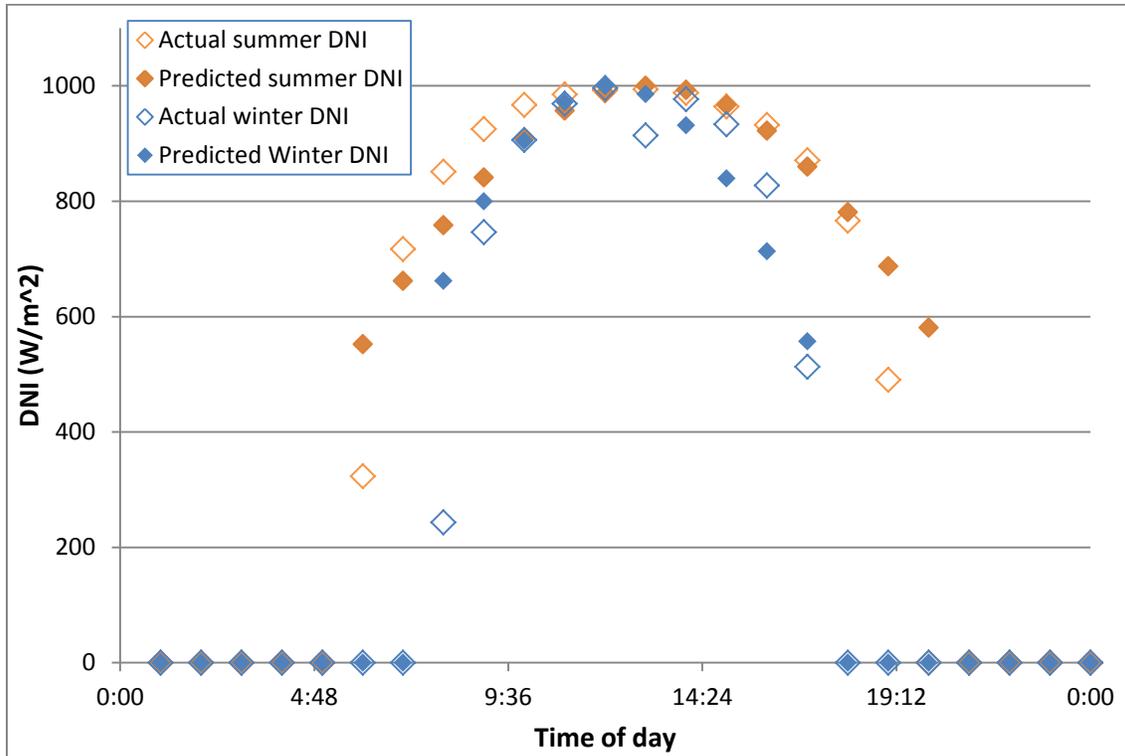
Figure 4 - Fit functions modeling normalized DNI vs. hour. Cosine was chosen to profile empirical data.

5.3 Reflectance

Panel reflectivity can be varied for each time step to account for the position of the sun relative to the array. Smooth glass and light textured glass with and without Anti-Reflection coating, along with deeply textured glass were analyzed to derive accurate functions for computing reflectivity based on sun incidence angle [7].

Table 1 contains the fit functions for panel reflectivity.

Table 1 - Reflectance fit functions for PV cover types.

PV Glass Cover Type	Fit Function Defined over $0° \leq \theta \leq 60°$	Fit Function Defined over $60° < \theta < 90°$
Smooth Glass without Anti-Reflection Coating	$y = 1.1977E\text{-}5\ x^2 - 9.5728E\text{-}4\ x + 4.410E\text{-}2$	$y = 6.2952E\text{-}5\ e^{0.1019x}$
Smooth Glass with Anti-Reflection Coating	$y = 1.473E\text{-}5\ x^2 - 9.6416E\text{-}4\ x + 3.2395E\text{-}2$	$y = 4.7464E\text{-}5\ e^{0.1051x}$
Light Textured Glass without Anti-Reflection Coating	$y = 1.5272E\text{-}5\ x^2 - 1.1304E\text{-}3\ x + 4.305E\text{-}2$	$y = 7.3804E\text{-}5\ e^{0.0994x}$
Light Textured Glass with Anti-Reflection Coating	$y = 1.4188E\text{-}5\ x^2 - 1.0326E\text{-}3\ x + 3.9016E\text{-}2$	$y = 7.0179E\text{-}5\ e^{0.0994x}$
Deeply Textured Glass	$y = 6.8750E\text{-}6\ x^2 - 6.5250E\text{-}4\ x + 2.10E\text{-}2$	$y = 4.1793E\text{-}5\ e^{0.0834x}$

5.4 Slope Error

The slope error can be automatically correlated with the selected surface type by checking *correlate slope error with module surface type*. If unchecked, the slope error can be entered manually. If checked, the following table is referenced for determining the appropriate slope error and corresponding value of β, the subtended beam angle:

Table 2. Slope error and beam spread vs. surface type

PV Glass Cover Type	Average RMS Slope Error (mrad)	Average Beam Spread (mrad)	Standard deviation of slope error	Standard deviation of beam error
Smooth Glass without Anti-Reflection Coating	6.55	87.9	4.43	53.3
Smooth Glass with Anti-Reflection Coating	8.43	110	2.58	30.9
Light Textured Glass without Anti-Reflection Coating	9.70	126	2.78	33.3
Light Textured Glass with Anti-Reflection Coating	9.16	119	3.17	38.0
Deeply Textured Glass	82.6	1000	N/A	N/A

5.5 Subtended Beam Angle

The glare analysis must account for the actual visible area of the PV array when viewed from the observation point. For example, less viewable area will be apparent when viewing an array with panel tilt of 0 degrees on a flat surface from the side than when viewing it from above in an aircraft.

To account for this, the analysis replaces the solar beam angle computed in Section **Error! Reference source not found.** with an array-limiting beam angle if the latter is a smaller value. This represents the physical situation where the sun beam "overflows" the PV array from the viewer's perspective, and thus less glare is possible.

$$\theta = \frac{1}{d} \sqrt{\frac{4 * A * \left|\cos \theta_{ref-pva}\right|}{\pi}}$$

where:

- A is area of PV array

- d is distance between observer and array

- $\theta_{ref-pva}$ is angle between reflected sun vector and PV array normal

6. Annual Energy Production

SGHAT can also predict the annual energy produced by a PV array based on its capacity and configuration. First the rated capacity is scaled at each time step based on the angle between the panel normal and the position of the sun. E.g. when the sun vector is perpendicular to the panel normal, the power produced will be the rated capacity.

$$P = P_{rated} * \cos \theta_{inc}$$

Next, this power is multiplied by the scaled time increment to get the energy produced in that time interval (kWh).

$$E_t = P * \frac{t}{60}$$

Finally, the energy produced over the year is summed to get the maximum annual energy produced by the array, assuming clear sunny skies each day.

$$E_{max} = \Sigma E_t$$

7. Other Formulations

7.1 Flight Path Calculations

The flight path OP coordinates are computed based on the latitude and longitude of the selected threshold, and the specified direction of the flight path.

First, the distance covered by one degree of longitude is calculated, based on the latitude.

$$d = radius_{earth} * \cos(lat_{thres})$$

Next, the distance between each point in terms of latitude and longitude is computed based on the direction and distance, in meters, of a degree of latitude or longitude. This is the Δlatitude and Δlongitude between each OP.

$$\Delta lat = \frac{402.3 * \cos \theta}{111325}$$

$$\Delta lng = \frac{402.3 * \sin \theta}{d}$$

Here d is the distance covered by one degree of longitude, 402.3 is ¼ mile in meters, and θ is the flight path direction.

Finally, compute each OP position by augmenting the coordinates of the previous OP by Δlat and Δlng.

The flight path heights of each OP are calculated based on the threshold height above ground, glide slope and threshold elevation. The tangent of the glide slope, multiplied by the distance from the threshold yields the height above the threshold of the given OP. Since each OP elevation is queried automatically from Google, this height value is augmented by the elevation difference between the OP and the threshold elevation.

$$height = distance * \tan(\varphi) + height_{thres} + (elevation_{thres} - elevation_{OP})$$

where φ is the glide slope.

8. Acknowledgments

9. References

[1]   Ho, C.K., C.M. Ghanbari, and R.B. Diver, 2011, Methodology to Assess Potential Glint and Glare Hazards From Concentrating Solar Power Plants: Analytical Models and Experimental Validation, *Journal of Solar Energy Engineering-Transactions of the Asme*, **133**(3).

[2]   Duffie, J.A. and W.A. Beckman, 1991, *Solar engineering of thermal processes*, 2nd ed., Wiley, New York, xxiii, 919 p.

[3]   Ho, C.K., *Relieving a Glaring Problem*, in *Solar Today*2013, American Solar Energy Society: Boulder, CO. p. 28 - 31.

[4]   Weisstein, Eric W. "Reflection." From *MathWorld* - A Wolfram Web Resource. http://mathworld.wolfram.com/Reflection.html

[5]   http://en.wikipedia.org/wiki/Line-plane_intersection

[6]   http://matplotlib.org/1.2.1/api/path_api.html#matplotlib.path.Path.contains_points

[7]   Yellowhair, J. *Reflectance Measurements on the Photovoltaic Sample Panels*, October 7, 2013.

[8]   Stine, W. B. and Geyer, M, 2001, *Power From the Sun*, http://www.powerfromthesun.net/book.html

Additional references can be found at www.sandia.gov/glare.